EurJOC European Journal of Organic Chemistry

FULL PAPER

DOI: 10.1002/ejoc.201201502

Turning-on the Quenched Fluorescence of Azomethines through Structural Modifications

Satyananda Barik[a][‡] and William G. Skene*[a]

Keywords: Fluorescence / Fluorescent probes / Donor–acceptor systems / Conjugation / Structure–activity relationships

A series of fluorene azomethines were prepared to examine the effect of structural modification on the absolute fluorescence quantum yields (Φ_{fl}). The change in fluorescence occurring upon reversing the orientation of the azomethine bond, the number of fluorene units, and alkylation at the 9,9′-positions of fluorene was examined. It was found that Φ_{fl} could be tailored with these structural modifications with $0.05 \leq \Phi_{fl} \leq 0.45$. The highest Φ_{fl} was measured for the trimer derived from 2,7-diamino fluorene with each fluorene being alkylated at the 9,9′-positions. The fluorescence quantum yields did not increase at 77 K, implying the absence of fluorescence quenching modes involving internal conversion. Fluorescence enhancement was also not observed upon protonating the imine with trifluoroacetic acid. This confirms that Waldon inversion and isomerization are not fluorescence deactivation modes. Additionally, no photoisomerization was observed either at room temperature or at 77 K when the fluorene derivatives were irradiated at 354 nm. In contrast, the *Z* photoisomer of a *N*-benzylideneaniline analogue was spectroscopically detected both by absorbance and by ^{1}H NMR spectroscopy.

Introduction

Conjugated materials prepared from azomethines (–N=C–) are interesting alternatives to their vinylene counterparts.[1] This is, in part, due to their isoelectronic properties relative to their carbon analogues.[2] More importantly, they have the advantage of ease of synthesis without the need for stringent reaction conditions or metal catalysts. Azomethines can also be easily purified without hydrolysis and they exhibit good thermal and reductive resistance in addition to being air stable.[3]

Although their interesting optical and electrochemical properties are suitable for use in plastic electronics, most azomethines are nonfluorescent.[4] Their quenched fluorescence is problematic for use of these materials in sensing applications and as emitting layers in organic light-emitting diodes.[5] As a result, much effort has been devoted to understanding the fluorescent deactivation processes of azomethines, with the ultimate aim of designing and developing fluorescent materials.[6] Intramolecular photoinduced electron transfer between the fluorophore and azomethine, in addition to nonradiative deactivation involving bond rotations, have been identified as efficient inherent fluorescence quenching modes of azomethines.[7] Theoretical and experimental studies further confirmed that photoisomerization of the thermodynamically stable *E* to the *Z* isomer also competes with fluorescence.[8] In most cases, the *Z* isomer is unstable and thermally reverts to the *trans* isomer as a result of a low $Z \rightarrow E$ isomerization activation barrier (ca. 70 kJ/mol).[9]

Whereas the main deactivation modes that are primarily responsible for quenching azomethine fluorescence have been identified, this knowledge has not led to the successful preparation of fluorescent conjugated azomethines. We were therefore motivated to prepare the series of conjugated azomethines shown in Scheme 1 to examine the structural effects on the fluorescence quantum yield (Φ_{fl}). These compounds were targeted because the effect of their different degrees of conjugation, alkylation at the 9,9′ positions, and orientation of the azomethine bond on the fluorescence properties could be examined. The fluorene derivatives were chosen because of their inherent fluorescence and their relevance for sensing and plastic electronic applications.[10] It was surmised that the collective structural effects could suppress the known and undesired singlet excited deactivation modes, notably internal conversion by bond rotation, and restore the inherent fluorene fluorescence. As a result, the preparation and photophysical and electrochemical characterization of the fluorene azomethine derivatives **1**–**9** are herein presented, with particular attention being devoted to Φ_{fl}. The fluorenylazomethines are additionally compared to their benzylimine derivatives **10** and **11**, which are known to photoisomerize.

[a] Laboratoire de caractérisation photophysique des matériaux conjugués, Département of chimie, Université de Montréal, Pavillon J. A. Bombardier, C. P. 6128, succ. Centre-ville, Montreal, QC, H3C 3J7, Canada
E-mail: w.skene@umontreal.ca
Homepage: www.groupskene.com
[‡] Current address: Institute of Chemical and Engineering Sciences
1 Pesek Road, Jurong Island, Singapore 627833, Singapore

Supporting information for this article is available on the WWW under http://dx.doi.org/10.1002/ejoc.201201502

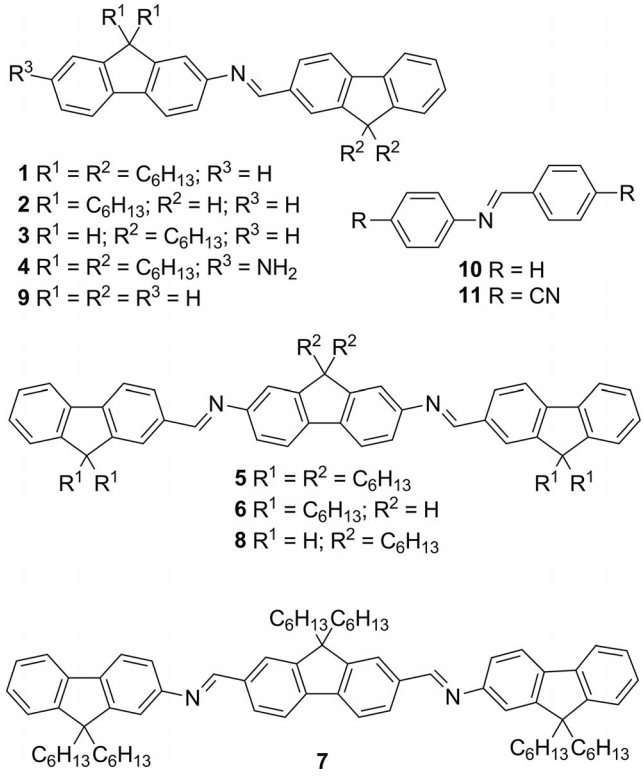

Scheme 1. Fluorene azomethine derivatives prepared and examined.

Results and Discussions

Photophysical Properties

Fluorenylazomethine derivatives were targeted because of the inherent fluorescence of fluorene, the Φ_{fl} of which is greater than 0.7.[11] Fluorene is also of particular interest because it is the most commonly used derivative that is used as an emitting layer in organic light-emitting diodes.[12] Fluorescent fluorenylazomethines would be beneficial not only because of their fluorescence, which could potentially be exploited for sensing applications and plastic electronics, but also for their ease of preparation. The derivatives shown in Scheme 1 were therefore prepared and examined. The azomethine derivatives were prepared by condensing the corresponding amine and aldehydes in appropriate stoichiometric amounts. The condensation reactions were performed under mild conditions by stirring at room temperature in ethanol together with a catalytic amount of trifluoroacetic acid. This is in contrast to standard methods used for the preparation of azomethines, which involve highly reactive titanium tetrachloride in anhydrous toluene.[13] The required aminofluorene derivatives were prepared from native fluorene first by 9,9′-dialkylation using standard methods,[14] followed by nitration using fuming HNO_3 and subsequent reduction over Pd/C and hydrazine hydrate. Owing to the instability of the 2-amino-9,9′-dialkylated derivatives, they were immediately reacted with the corresponding aldehydes to form hydrolytically, oxidatively, and reductively robust azomethines.

The absorbance and fluorescence spectra of **1**–**9** were measured in dichloromethane, and the corresponding data are found in Table 1. Given that the dimers and trimers differ in their degree of conjugation, this was expected to affect both the absorbance and fluorescence spectra. As shown in part A of Figure 1, dimers **1**–**3** consistently absorb at ca. 360 nm, regardless of substitution at the 9,9′-positions. The exception is **4**, which is bathochromically shifted by 30 nm owing to the electron-donating effect of the amine. The absorbances of the trimers were all redshifted

Table 1. Photophysical and electrochemical properties of fluorenylazomethines measured in dichloromethane.

	λ_{abs} [nm]	λ_{fl} [nm][a]	Φ_{fl} 298 K[b] (H^+)	Φ_{fl} 77 K	E_{pa} [V][c]	HOMO [eV][d]	LUMO [eV][e]	E_g^{opt} [eV][f]	E_g^{el} [eV][g]
1	362	416	0.15 (0.17)	0.19	0.92	5.14	2.48	2.7	2.7
2	362	425	0.05 (0.08)	0.07	0.91	5.18	2.47	2.7	2.7
3	363	452	0.07 (0.09)	0.09	0.90	5.17	2.43	2.7	2.7
4	391	552	0.09 (0.03)	0.05	0.86	5.16	2.56	2.6	2.6
5	398	505	0.45 (0.47)	0.78	0.83	5.12	2.54	2.6	2.5
6	392	453	0.05 (0.06)	0.08	0.93	5.18	2.52	2.7	2.6
7	398	455	0.11 (0.12)	0.16	0.95	5.21	2.60	2.6	2.6
8	390	451	0.07 (0.08)	0.09	0.96	5.24	2.60	2.6	2.6
9	361	445	–[h]	–[h]	1.53	5.60	2.70	2.9	2.9

[a] Fluorescence measured upon excitation at the corresponding absorbance maximum. [b] Absolute fluorescence quantum yield at room temperature. Values in parentheses are absolute quantum yields measured upon azomethine protonation with TFA. [c] Oxidation potential relative to saturated Ag/Ag^+ electrode. [d] Relative to the vacuum level. [e] LUMO = HOMO – E_g^{opt}. [f] Spectroscopically determined energy gap taken from the absorbance onset ($E_g = 1240/\lambda_{onset}$). [g] Electrochemically derived energy gap. [h] Insufficient solubility for accurate absolute Φ_{fl} measurements.

by 30 nm relative to the corresponding dimers, which is a result of the increased degree of conjugation courtesy of the additional azomethine bond. The absorbance of the trimers was slightly influenced by the alkylation at the 9,9′-positions, unlike the dimers. For example, the absorbance of both the fully alkylated derivatives **5** and **7** is redshifted by 8 nm relative to **8**. The observed shift is a result of the weak electron-donating effect of the alkyl group.

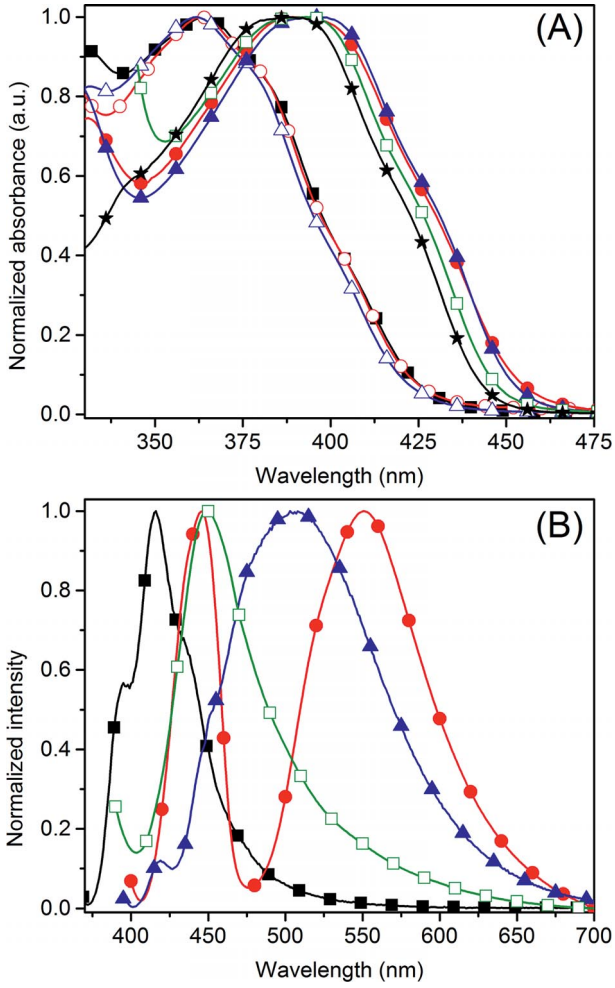

Figure 1. (A) Normalized absorbance spectra of **1** (filled black square), **2** (open red circle), **3** (open blue triangle), **4** (filled red circle), **5** (filled blue triangle), **7** (open green square), **8** (black star) measured in dichloromethane. (B) Normalized fluorescence spectra of **1** (filled black square), **4** (filled red circle), **5** (filled blue triangle), and **7** (open green square), measured in dichloromethane by excitation at the corresponding absorbance maximum.

Fluorescence spectra are more sensitive than absorbance spectra to both the fluorene alkylation and the orientation of the azomethine bond. As shown in Table 1, the fluorescence of **2** is bathochromically shifted by 10 nm relative to **1**, and **3** is further redshifted by 30 nm. Electron-rich **4** undergoes the most pronounced redshift of 135 nm relative to **1**. This is, in part, due to the intramolecular charge transfer that takes place between the terminal electron-donating and azomethine electron-withdrawing groups, which is evidenced by the appearance of two peaks in the emission spectrum. Whereas the trimers are bathochromically shifted by 40 nm compared with dimer **1**, there are only small spectral changes between them. The exception is all-alkylated **5**, which is redshifted by 50 nm relative to the other trimers. Given that the only difference between **5** and **7** is the orientation of the azomethine bond, this is most likely responsible for the difference in their fluorescence. The redshift observed for **5**, concomitant with its larger Stoke shift, implies that it has a more polar excited state than **7**. Similarly, **1** and **3** differ only in the orientation of the azomethine bond. The 50 nm difference between their fluorescence peaks can also be assigned to the orientation of the azomethine bond.

The azomethine property that is of particular interest is the fluorescence quantum yield Φ_{fl}. These values were measured with an integrating sphere, which provides absolute measurement values that are independent of a reference.[15] The absolute Φ_{fl} of **1**–**9** were subsequently determined by using an integrating sphere. According to Table 1, substitution at the 9,9′-positions affects the Φ_{fl}. For example, $\Phi_{fl} < 0.10$ was measured for all compounds containing an unalkylated fluorene. The Φ_{fl} increased to 0.15 when the fluorene was alkylated as with **1**. The highest value was measured with **5**, the Φ_{fl} of which was nearly ten times greater than its geometric analogue **7**. The different Φ_{fl} for the geometric analogues suggests that the orientation of the azomethine significantly alters the dipole moment, which, in turn, affects the fluorescence emission. The collective data and the image in Figure 2 clearly demonstrate that the fluorescence quenching deactivation pathways of azomethines can be suppressed with subtle structural modifications involving alkylation at the 9,9′-positions and by altering the orientation of the azomethine bond. The net effect is fluorescent azomethines, especially when they are prepared from the diamino fluorene derivative **14**. This is in contrast to other fluorenylazomethines, the emission yields of which are so low that their Φ_{fl} cannot be measured.[16]

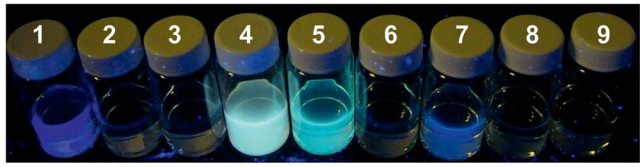

Figure 2. Combined picture showing the fluorescence of **1**–**9** (from left to right) in dichloromethane upon irradiation with a UV lamp at 254 nm.

Cryofluorescence

The cryofluorescence of **1**–**9** was investigated to further study the fluorescence deactivation modes. Deactivation processes occurring by internal conversion such as bond rotation can be identified with low temperature fluorescence.[17] Such deactivation processes are suppressed at reduced temperatures, resulting in increased fluorescence. In contrast, singlet excited state deactivation by intersystem crossing to the triplet state is a temperature-independent inherent property.[17b,18] Cryofluorescence was performed in

2-methyltetrahydrofuran and methylcyclohexane at 77 K. The low-temperature Φ_{fl} value for the compounds was calculated from the absolute room temperature values after taking into account the temperature-dependent refractive index change of the solvent. Variable-temperature fluorescence was also measured at discrete intervals between 300 and 180 K, as shown in the inset of Figure 3B. The lower temperature limit for the cryofluorescence measurements was 10 K above the solvent freezing point to avoid the large solvent volume change that takes place at the solvent freezing point. This could potentially crack the cuvette during the measurements. In all cases, the Φ_{fl} increased by about 30% at 77 K. Whereas the Φ_{fl} of **1**–**4**, and **6**–**9** could be increased to 0.1, the most noticeable increase was for **5**, the Φ_{fl} of which increased to 0.78 at 77 K. This is consistent with the Φ_{fl} of native fluorene. Whereas rapid intramolecular deactivation modes such as PET and photoisomerization (see below) along with intrinsic intersystem crossing to the triplet state cannot be unequivocally excluded as singlet excited state deactivation modes, the temperature-dependence studies confirm that azomethine fluorescence quenching does not occur by bond rotation resulting in different rotamers or internal conversion. Moreover, the ca. 50% increase in Φ_{fl} observed for **5** at low temperature implies that it is significantly deactivated by internal deactivation while still being inherently fluorescent at room temperature. Of particular interest is the absence of Φ_{fl} increase upon protonating the azomethine with trifluoroacetic acid (TFA). It was previously shown that azomethine protonation resulted in fluorescence enhancement, which occurred by suppression of both Waldon inversion of the nitrogen and photoisomerization.[19] The lack of increased Φ_{fl} with protonation suggests that these two deactivation modes are not responsible for the quenched fluorescence of the studied fluorenylazomethines.

The temperature-dependent fluorescence of **5** was additionally examined in different solvents to assess the effect of polarity on the fluorescence. It was found that although the fluorescence quantum yields did not change with polarity, the fluorescence spectra were affected differently as a function of temperature in the different solvents. As can be seen in Figure 3 (A), the fluorescence of **5** bathochromically shifts by up to 25 nm with decreasing temperature in 2-methyltetrahydrofuran. The same trend was observed in dichloromethane. This trend is ascribed to the lower energy rotamer being adopted at low temperatures, which is assumed to be an all-*anti*-rotamer. In contrast, no temperature-dependent spectral shifts were observed for **5** in methylcyclohexane. The redshift in the fluorescence observed in polar solvents implies that the excited state has a high dipole moment. Given that this trend was not observed with the other azomethines investigated, the increased excited state polarity is most likely a result of the orientation of the azomethine bond in **5**. The orientation of the azomethine was previously shown to affect the fluorescence quantum yields, with $\Phi_{fl} \approx 0.5$ being observed with unidirectional azomethines.[20] This is in contrast to polyfluorenylazomethines having bidirectional azomethines similar to **4** and **5**, the fluorescence of which is reduced by half ($\Phi_{fl} < 0.25$).[19,21] The collective temperature-dependent fluorescence data provide evidence that internal conversion is responsible for quenching the fluorenylazomethine fluorescence, albeit only up to a maximum of 30%.

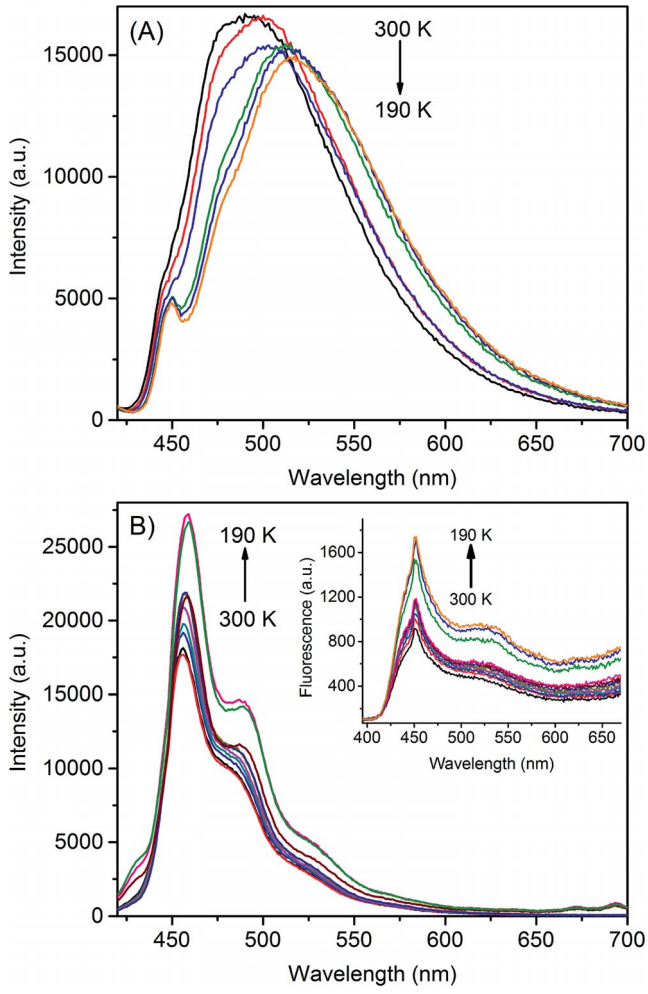

Figure 3. Cryofluorescence of **5** measured between 300 and 190 K in (A) deaerated 2-methyltetrahydrofuran, and (B) methylcyclohexane. Inset: cryofluorescence of **2** measured between 300 and 190 K in deaerated dichloromethane.

Isomerization

Fluorescence deactivation of the azomethines by photoisomerization from the *E* to the *Z* isomer was also investigated. Significant changes in both the absorbance and fluorescence spectra are expected for the two isomers. More specifically, the reduced degree of conjugation of the *Z* isomer should result in hypsochromic shifts in both the absorbance and fluorescence spectra. Changes in the absorbance spectra upon irradiating benzylimines **10** and **11** were first examined. These were chosen as reference compounds because they are known to photoisomerize. Furthermore, their *Z* isomer is thermally stable at room temperature, allowing it to be spectroscopically observed by standard absorbance spectroscopy.[8a] Given that **10** and **11**

are nonfluorescent, only their absorbance spectra were examined. As shown in Figure 4 (A), significant spectral differences occur upon irradiating **10** and **11** at 365 nm for 5 min, with a blueshifted shoulder appearing for **10** at 290 nm. Moreover, the entire spectrum of **11** is hypsochromically shifted by 15 nm upon irradiation at room temperature. Formation of the *Z* isomer upon irradiation of **11** was also unequivocally confirmed by ^{1}H NMR spectroscopic analysis. As shown in the inset of Figure 5 (A), **11** has only one imine, according to the singlet at δ = 8.775 ppm for the *E* isomer. This is assumed to be the thermodynamically stable *E* isomer. Evidence of a new product being formed upon irradiation comes from the splitting of the peaks in the NMR spectrum (Figure 5, B). This photoproduct is assigned to the *Z* isomer, according to the new imine singlet at δ = 8.768 ppm. The upfield shift of the *Z* imine proton is a result of its decreased degree of conjugation relative to the *E* isomer.

Isomerization studies were undertaken with **2** and **5**, which were chosen because of their respective low and high Φ_{fl}. It was expected that **2** would show significant spectral changes similar to those of **11**, providing that its low Φ_{fl} is a result of efficient photoisomerization.[22] Compound **5** was chosen as a benchmark to ensure that the irradiation conditions used did not induce any photodecomposition. Interestingly, no changes in the absorbance or fluorescence spectra of either **2** or **5** were observed upon irradiation at 365 nm even for prolonged times of 24 h at room temperature. No spectral changes were observed at 77 K, the temperature at which even the most thermally unstable *Z* isomer should be trapped (Figure 4, B). Compound **2** was also irradiated in both deuterated acetone and methylcyclohexane to verify the absence of photoisomerization by NMR spectroscopy. Similar to **11**, a new downfield shifted imine proton should be observed if the Z isomer of **2** is formed upon photoisomerization. Unirradiated **2** was used as a benchmark for assigning the imine proton of the *E* isomer. There are no noticeable differences between the unirradiated and irradiated samples of **2**. It should be noted that the baseline peaks in the samples are contaminants and do not arise from *E*/*Z* isomers. As shown in the insets C and D of Figure 5, there is no change in the ratio of the protons and no new protons appear in the imine region. The NMR spectra confirm that the *Z* isomer is not produced upon photoirradiation. The absence of aldehyde peaks in the spectra further confirms that **2** does not photodecompose.

The collective spectral irradiation data of **2** and **5** confirm that the fluorene azomethines do not photoisomerize, unlike their benzylimine counterparts.[8a,8b,23] The absence of a spectroscopically visible *Z* isomer may be due to a short lifetime because of a low thermal $Z \rightarrow E$ activation or from a phantom state. However, this can be excluded because the $Z \rightarrow E$ thermal activation barrier of **2** is expected to be much larger than that of **11**. This is a result of the alkyl groups and larger aromatic core, which collectively increase the entropic contributions, requiring longer lifetimes for the intramolecular arrangements associated with isomerization. Further evidence against isomerization was provided by the fluorescence lifetime and quantum yield measurements in ethylene glycol (see the Supporting Information). The isomerization should be significantly reduced in this viscous solvent, resulting in increased fluorescence lifetime and enhanced Φ_{fl}, providing the $E \rightarrow Z$ conversion occurs via the singlet manifold.[24] However, no change in the fluorescence lifetime or quantum yield was observed between ethylene glycol and dichloromethane. Deactivation of the singlet excited states of fluorenylazomethines therefore most likely occurs by other nonradiative means, unlike their benzylimine counterparts. Intersystem crossing to form the triplet state can also be discounted because no visible triplet of arylazomethines has been reported for analogous fluor-

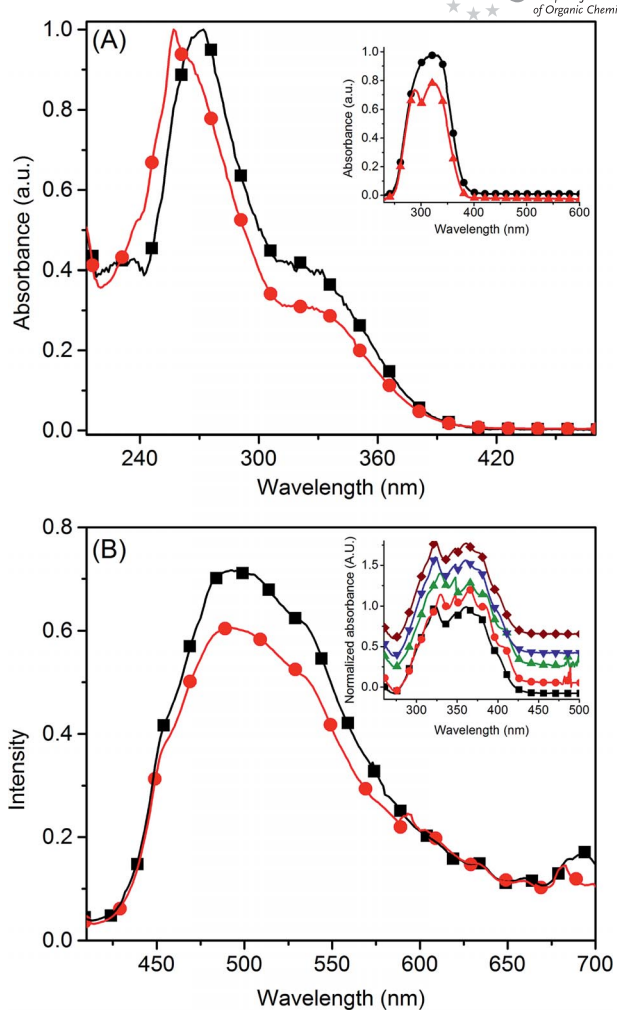

Figure 4. (A) Absorbance spectra of **11** in methylcyclohexane prior to (filled black square) and after (filled red circle) irradiation at 365 nm for 30 min at room temperature. Inset: absorbance spectra of **10** in methyl-cyclohexane prior to (filled black square) and after (filled red triangle) irradiation at 365 nm for 30 min at room temperature. (B) Fluorescence spectra of **2** prior to (filled black square) and after (filled red circle) irradiation at 365 nm for 30 min at room temperature in cyclohexane. Inset: absorbance spectra of **2** at room temperature prior to (filled black square) and after irradiating for 30 min (lilac filled diamond), 77 K (filled red circle), irradiating at 77 K for 30 (filled green triangle) and 60 (inverted filled blue triangle) min. The offset between the spectra is for visual purposes only.

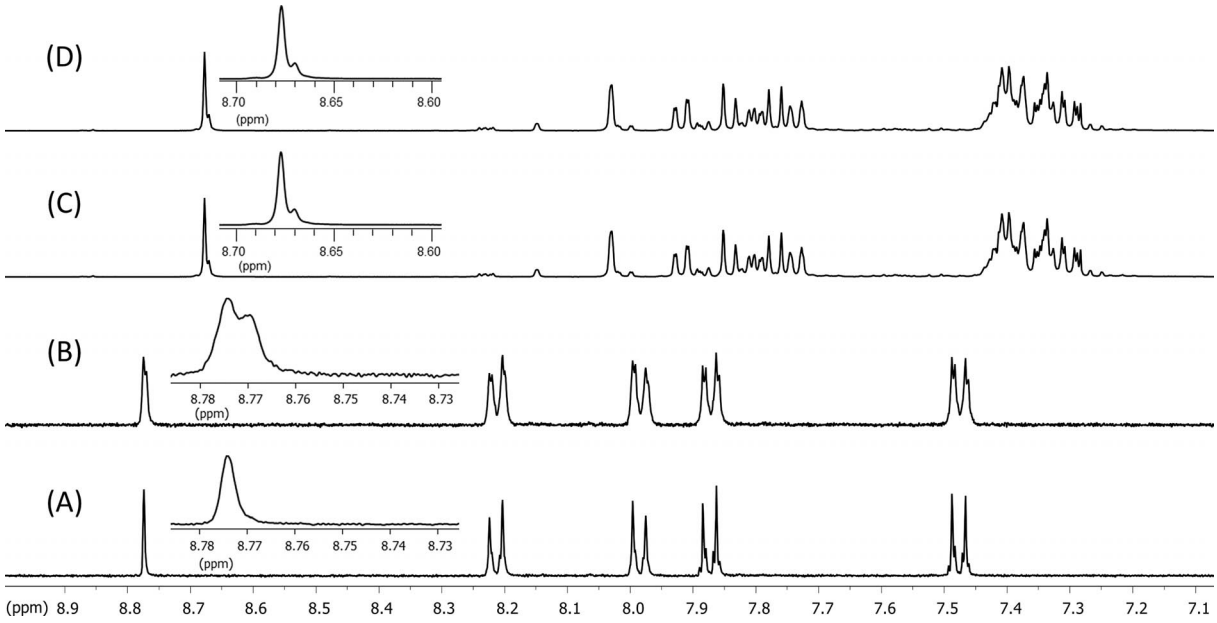

Figure 5. ^{1}H NMR spectra of **11** prior to (A) and after (B) irradiation at 365 nm for 5 min at room temperature in deuterated acetone. ^{1}H NMR spectra of **2** prior to (C) and after (D) irradiating at 365 nm for 24 h at room temperature in deuterated acetone. The insets show the expanded imine region.

enylazomethines.[7c,25] The collective fluorescence and irradiation data provide indirect evidence that rapid intramolecular deactivation processes, such as intramolecular photoinduced electron transfer between the fluorophore and the azomethine, and internal conversion, among others, are responsible for fluorescence quenching of the fluorenylazomethines. These deactivation processes are nonetheless reduced with **5**, resulting in appreciable fluorescence.

Electrochemical Properties

The electrochemical properties of the fluorenylazomethines were investigated by using cyclic voltammetry to further study the effect of alkylation and degree of conjugation. The electrochemical measurements were performed in dichloromethane at a scan rate of 100 mV/s. The fluorenylazomethines were found to undergo a one-electron oxidation that was quasi-reversible, as shown in Figure 6, by using equimolar amounts of ferrocene as an internal reference. The exception is **4**, which underwent two reversible one-electron oxidations at 620 and 880 mV. The quasi-reversibility is a result of the reactive radical cation, which is known to undergo cross-coupling. The terminal amine of **4** prevents such reactions, resulting in the observed reversible oxidation. The reversible oxidation of **4** also confirms the stability of the azomethine connection towards oxidation. Moreover, the oxidation potentials (E_{pa}) of **1**–**9** were found to be consistently ca. 930 mV and they varied only by 30 mV, contingent on structure. The absence of significant variation of E_{pa} between the dimer and trimers is not surprising because the electron-withdrawing effect of the azomethines offsets any reduction in the E_{pa} that arises from the increased degree of conjugation of the trimers. However, less positive E_{pa} values were found for **4** and **5** due to the electron-donating terminal amine and orientation of the azomethine bond, in addition to the multiple alkylations, respectively. The effect of the azomethine orientation on the oxidation potential is further confirmed by the 120 mV E_{pa} difference between **5** and **7**. Because electron-withdrawing groups influence the reduction and not the oxidation potentials, the observed E_{pa} between **5** and **6** confirms that the

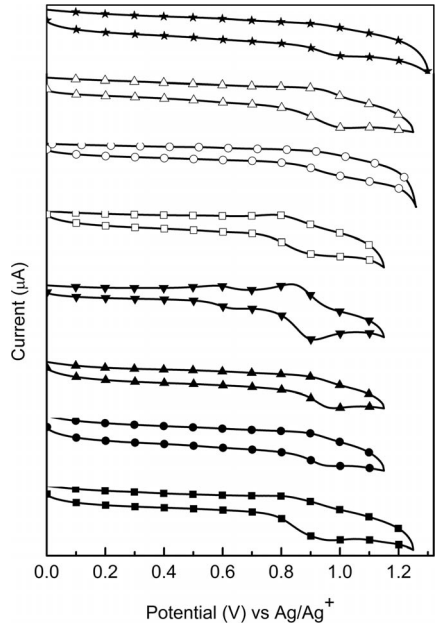

Figure 6. Anodic cyclic voltammograms of **1** (filled square), **2** (filled circle), **3** (filled triangle), **4** (inverted filled triangle), **5** (open square), **6** (open circle), **7** (open triangle), **8** (star) measured in deaerated dichloromethane.

different dipole moments caused by the azomethine orientation significantly perturb the HOMO energy levels. The electrochemical data further confirm the air stability of the azomethine derivatives examined because their E_{pa} values are much higher than the reduction potential of oxygen.

Given the potential use of the fluorenylazomethines derivatives in electronic devices, their HOMO and LUMO energy values, in addition to their energy gaps (E_g), must be compatible with commonly used device electrodes. As a result, these energy values were calculated from the electrochemical data by standard methods from the oxidation and reduction potential onsets.[26] This were calculated according to the following equations: HOMO = 4.4 + E_{pa}^{onset} and LUMO = HOMO – E_g^{opt}, where E_{pa}^{onset} and E_g^{opt} are the oxidation potential onset and optical energy gap, respectively. The calculated HOMO and LUMO energy values were consistently 5.2 and 2.5 eV, respectively (Table 1). The energy gap was calculated from the corresponding HOMO and LUMO energy values and they were also consistent (2.6 ± 0.1 eV) regardless of structure. The measured E_g values are lower than their fluorenyl polymer analogues (E_g = 3.0 eV).[27] There is also good correlation between the spectroscopically (E_g^{opt}) and electrochemically (E_g^{el}) determined energy gaps. This confirms that the electrochemically measured oxidation and reduction processes correspond to radical cation and anion formation, respectively, and not to reduction of the azomethine or to oxidative decomposition.

The stabilities of the electrochemically produced radical cations were additionally investigated by spectroelectrochemistry. The measurements were performed in dichloromethane with 0.3 M tetrabutylammonium hexafluorophosphate as the electrolyte. The resulting spectral changes were observed by applying a potential slightly more positive than the corresponding E_{pa} of the given azomethine. In all cases, the absorbance of the generated radical cation was bathochromically shifted from the corresponding neutral form. The most stark visible color change was with **7**, whose color changed from yellow to orange upon oxidation at 1.4 V, as shown in the inset of Figure 7. The new absorbance at 540 nm corresponds to the electrochemically generated radical cation. The oxidized state could be neutralized by applying a potential of 0 V. Repeated switching between the oxidized and neutral states was possible by applying 1.4 and 0 V, respectively, without detectable color fastening. The consistent color demonstrates the robustness of the azomethines towards oxidation.

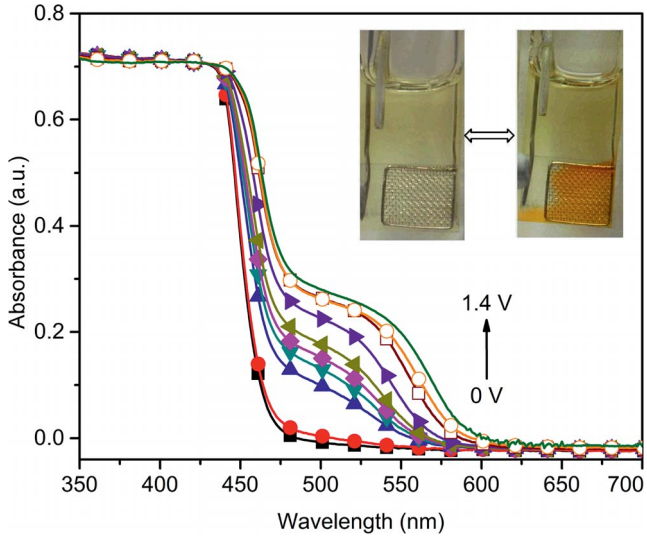

Figure 7. Spectroelectrochemistry of **7** recorded in deaerated dichloromethane at 0 (filled black square), 0.8 (filled red circle), 0.9 (blue filled triangle), 1.0 (inverted filled turquoise triangle), 1.1 (pink diamond), 1.2 (sideways left filled green triangle), 1.3 (sideways right filled blue triangle), 1.3 (open black square), 1.4 (open orange circle), 1.4 V (green line). Inset: color observed for the neutral (left) and oxidized (right) states at the platinum mesh electrode.

Conclusions

It was found that fluorenylazomethine derivatives could become fluorescent by both simple alkylation at the 9,9′-positions and by changing the orientation of the azomethine bond. More notably, the absolute quantum fluorescence yield increased from 10 to 48% with an all-alkylated trimer derived from 2,7-diamiofluorene. Temperature-dependent fluorescence studies confirmed that nonradiative deactivation modes accounted for less than 30% of the fluorescence quenching. Moreover, $E \rightarrow Z$ conversion through photoisomerization was further precluded as a viable singlet excited state deactivation mode. The collective spectroscopic data confirm that combinations of deactivation modes are responsible for fluorescence quenching of fluorenylazomethines. The inherent quenched fluorescence of azomethines can nonetheless be turned-on by structural modifications that suppress these fluorescence deactivation modes. The structurally induced fluorescence enhancement provides solid evidence that highly fluorescent azomethines are possible. This result demonstrates that these easily prepared materials have optical and electrochemical properties that are suitable for potential use as sensors and in plastic devices. Moreover, these compounds can withstand repeated oxidation/neutralization cycles. With additional structural modification and by including various electron-rich and electron-deficient moieties, highly fluorescent azomethines are expected to have discrete emissions over a broad range of wavelengths.

Experimental Section

Materials and Methods: Reagents and solvents were used as received from commercial sources unless otherwise stated. Anhydrous and deoxygenated solvents were obtained by passing through an activated alumina column system. ^{1}H and ^{13}C NMR spectra were recorded at room temperature with a 400 MHz spectrometer. All samples were dissolved in deuterated solvents and the spectra were referenced to the solvent line relative to TMS.

Spectroscopic Measurements: Absorbance measurements were made with a Cary-500 spectrometer and fluorescence studies were

carried out with an Edinburgh Instruments FLS-920 fluorimeter after thoroughly deaerating the samples with nitrogen for 20 min. Fluorescence spectra were obtained by exciting the solution at the maximum absorbance of the compound of study. Absolute quantum yields were measured with an integrating sphere by exciting at the maximum absorbance of the compound of study. Variable and discrete temperature fluorescence was obtained with an Oxford Instruments OptiStat DN cryostat. Fluorescence measurements at 77 K were performed with samples dissolved in either a 4:1 ethanol/methanol mixture or in dichloromethane. The temperature-dependent cryofluorescence measurements ranging between 77 and 190 K were performed in 2-methyltetrahydrofuran and methylcyclohexane. These solvents were chosen because of their capacity to form transparent and homogeneous glass matrices in liquid nitrogen.

Electrochemical Measurements: Cyclic voltammetry measurements were performed with a Bio-Logic potentiostat. The compounds were dissolved in anhydrous and deaerated dichloromethane at 10^{-4} M with 0.3 M $TBAPF_6$. A platinum electrode and a saturated Ag/AgCl electrode were employed as auxiliary and reference electrodes, respectively.

Photoirradiation: Samples were prepared in either quartz NMR tubes or spectroscopic cuvettes. For absorbance and fluorescence studies, the samples were prepared with an absorbance of less than 0.01 at an irradiation wavelength of 365 nm. Samples for NMR studies were prepared with an absorbance of greater than 2 at 365 nm. All samples were thoroughly deaerated by bubbling with nitrogen for a minimum of 20 min. The samples were sealed and then irradiated in a photoreactor having either two or four lamps for the prescribed time.

Syntheses: The precursors were obtained from commercial sources including 2-aminofluorene, 2,7-diaminofluorene, 2-formylfluorene, 2,7-fluorenedicarbaldehyde, benzaldehyde, aniline, 4-formylbenzonitrile, and 4-aminobenzonitrile. Compounds **12**–**20** were prepared as outlined in Scheme 2 according to previously reported procedures.[28]

Synthesis of Fluorenoazomethine Derivatives. General Procedure: The appropriate stoichiometric amounts of fluorene dialdehyde/monoaldehyde and fluorene diamine/monoamine were dissolved in ethanol (40 mL) and a catalytic amount of TFA (1.0 M, 50 μL) was added. The reaction mixture was stirred at room temperature for 16 h (Scheme S1 in the Supporting Information). The solvent was evaporated and the product was extracted into ethyl acetate. The organic layer was washed with brine solution and dried with Na_2SO_4. After removing the salt by filtration, the solvent was evaporated under reduced pressure and the crude product was purified by column chromatography over activated basic alumina using various hexanes/ethyl acetate mixtures as eluent.

(*E*)-*N*-[(9,9-Dihexyl-9*H*-fluoren-2-yl)methylene]-9,9-dihexyl-9*H*-fluoren-2-amine (1): Obtained from 9,9-dihexyl-9*H*-fluoren-2-ylamine (**16**; 110 mg, 0.31 mmol) and 9,9-dihexyl-9*H*-fluorene-2-carbaldehyde (**18**; 95 mg, 0.262 mmol). The title compound was obtained as a yellow solid (120 mg, 55%) after purification by column chromatography (hexane/ethyl acetate, 90:10). ^{1}H NMR ($CDCl_3$): δ = 8.67 (s, 1 H), 8.02 (s, 1 H), 7.91 (dd, 1 H), 7.83 (d, 1 H), 7.75 (m, 3 H), 7.29–7.40 (m, 8 H), 2.05 (dt, 8 H), 1.09 (m, 24 H), 0.8 (dt, 12 H), 0.69 (t, 8 H) ppm. ^{13}C NMR ($CDCl_3$): δ = 160.7, 152.4, 152.0, 151.9, 151.8, 151.2, 145.0, 141.2, 140.7, 139.7, 135.6, 129.3, 128.3, 127.3, 127.2, 123.4, 123.2, 122.8, 120.7, 120.6, 120.38, 120.3, 119.9, 119.8, 116.5, 55.7, 55.6, 41.0, 40.8, 32.0, 31.9, 30.2, 30.1, 24.2, 23.0, 14.4 ppm. HRMS (+ve): *m*/*z* calcd. for $[C_{51}H_{67}N + H]^+$ 694.5274; found 694.5276.

(*E*)-*N*-[(9*H*-Fluoren-2-yl)methylene]-9,9-dihexyl-9*H*-fluoren-2-amine (2): Obtained from 9,9-dihexyl-9*H*-fluoren-2-ylamine (**16**; 540 mg, 1.54 mmol) and 9*H*-fluorene-2-carbaldehyde (200 mg, 1.03 mmol). The title compound was obtained as a yellow solid (250 mg, 40%) after purification by column chromatography (hexane/ethyl acetate, 90:10). ^{1}H NMR ($CDCl_3$): δ = 8.66 (s, 1 H), 8.22 (s, 1 H), 7.88 (dd, 3 H), 7.73 (dd, 2 H), 7.62 (d, 1 H), 7.26–7.44 (m, 7 H), 4.01 (s, 2 H), 2.01 (t, 4 H), 1.07 (m, 12 H), 0.78 (t, 6 H), 0.69 (t, 4 H) ppm. ^{13}C NMR ($CDCl_3$): δ = 160.1, 152.4, 151.6, 151.2, 145.3, 144.6, 144.1, 141.4, 141.2, 136.7, 135.4, 129.0, 128.0, 128.0, 127.4, 127.1,

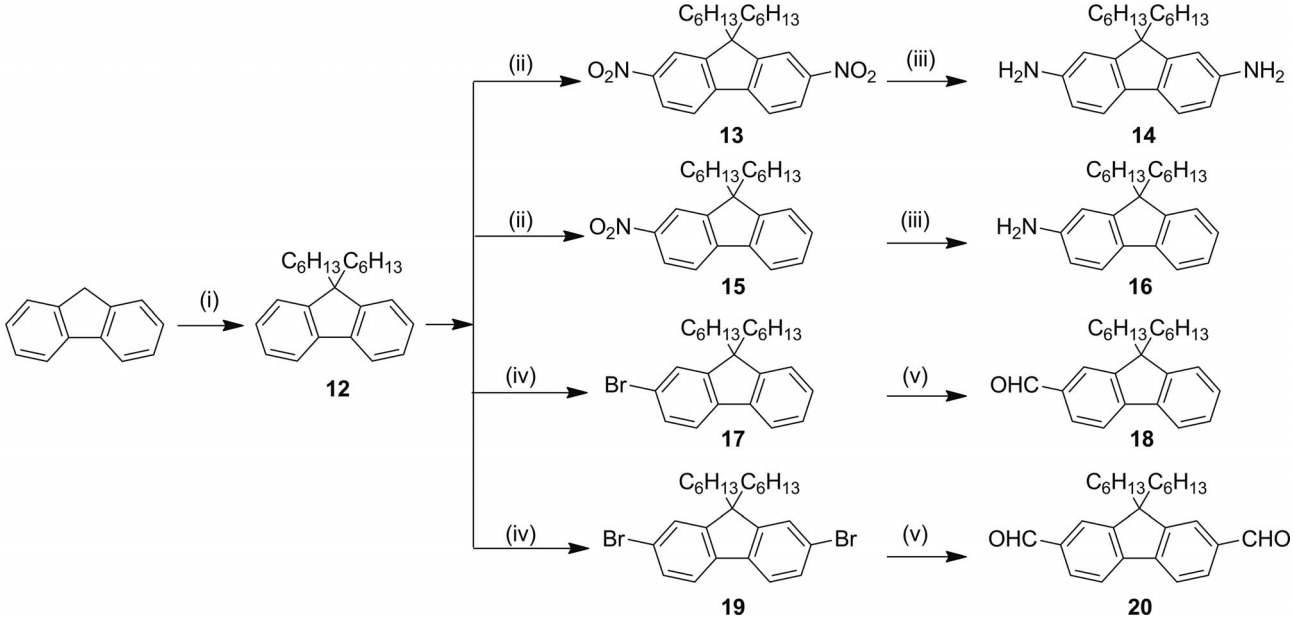

Scheme 2. Synthetic scheme used to prepare fluorenylazomethines. *Reagents and conditions*: (i) DMSO, 2 M NaOH, 1-bromohexane, phase-transfer catalyst, room temp., 2 d; (ii) AcOH, conc. HNO_3, reflux, 2 h; (iii) ethanol, THF, 10% Pd/C, hydrazine hydrate, reflux, 4 h; (iv) NBS, $CHCl_3$/AcOH (1:1), room temp., 18 h; (v) TMEDA, hexane, THF, BuLi, DMF, –78 °C, 16 h.

125.6, 125.1, 123.2, 120.9, 120.6, 120.4, 119.9, 119.6, 116.7, 55.6, 40.9, 37.2, 31.9, 30.1, 24.1, 23.0, 22.6, 14.4 ppm. HRMS (+ve): *m*/*z* calcd. for $[C_{39}H_{43}N + H]^+$ 526.3396; found 526.3392.

(*E*)-*N*-[(9,9-Dihexyl-9*H*-fluoren-2-yl)methylene]-9*H*-fluoren-2-amine (3): Obtained from 9*H*-fluoren-2-ylamine (120 mg, 0.662 mmol) and 9,9-dihexyl-9*H*-fluorene-2-carbaldehyde (**18**; 200 mg, 0.55 mmol). The title compound was obtained as a light-yellow solid (180 mg, 62%) after purification by column chromatography (hexane/ethyl acetate, 90:10). ^{1}H NMR ([D$_6$]acetone): δ = 8.64 (s, 1 H), 7.97 (s, 1 H), 7.76–7.88 (m, 5 H), 7.56 (d, 1 H), 7.49 (s, 1 H), 7.31–7.40 (m, 6 H), 3.97 (s, 2 H), 2.06 (t, 4 H), 1.1 (m, 12 H), 0.77 (t, 6 H), 0.65 (t, 4 H) ppm. ^{13}C NMR ($CDCl_3$): δ = 160.7, 152.0, 151.7, 144.9, 144.8, 143.7, 141.8, 140.7, 135.6, 129.2, 128.3, 127.3, 127.2, 127.1, 126.8, 125.4, 123.4, 122.9, 120.8, 120.7, 120.6, 126.5, 120.2, 120.1, 118.0, 56.1, 55.6, 40.7, 37.3, 31.9, 31.3, 30.1, 24.1, 22.9, 14.4 ppm. HRMS (+ve): *m*/*z* calcd. for $[C_{39}H_{43}N + H]^+$ 526.3396; found 526.3392.

(*E*)-*N*^{2}-[(9,9-Dihexyl-9*H*-fluoren-2-yl)methylene]-9,9-dihexyl-9*H*-fluorene-2,7-diamine (4): Obtained from 9,9-dihexyl-9*H*-fluorene-2,7-diamine (**14**; 170 mg, 0.411 mmol) and 9,9-dihexyl-9*H*-fluorene-2-carbaldehyde (**18**; 540 mg, 1.5 mmol). The title compound was obtained as a yellow solid (90 mg, 31%) after purification by column chromatography (hexane/ethyl acetate, 70:30). ^{1}H NMR ($CDCl_3$): δ = 8.67 (s, 1 H), 8.01 (s, 1 H), 7.9 (dd, 4 H), 7.5 (dd, 1 H), 7.28–7.39 (m, 7 H), 6.65 (d, 2 H), 3.75 (br. s, 2 H), 2.08 (t, 8 H), 1.09 (m, 24 H), 0.8 (t, 12 H), 0.70 (t, 8 H) ppm. ^{13}C NMR ($CDCl_3$): δ = 160.6, 159.9, 153.2, 152.6, 152.0, 150.3, 146.2, 140.7, 140.3, 139.5, 135.8, 132.6, 129.3, 129.2, 128.3, 128.2, 127.3, 123.4, 122.8, 120.7, 116.6, 116.5, 114.4, 110.2, 55.6, 55.3, 41.3, 40.8, 32.0, 31.9, 30.2, 30.1, 24.1, 23.1, 23.0, 14.4 ppm. HRMS (+ve): *m*/*z* calcd. for $[C_{51}H_{68}N_2 + H]^+$ 709.5383; found 709.5386.

(N^2*E*,N^7*E*)-*N*^{2},*N*^{7}-Bis[(9,9-dihexyl-9*H*-fluoren-2-yl)methylene]-9,9-dihexyl-9*H*-fluorene-2,7-diamine (5): Obtained from 9,9-dihexyl-9*H*-fluorene-2,7-diamine (**14**; 150 mg, 0.411 mmol) and 9,9-dihexyl-9*H*-fluorene-2-carbaldehyde (**18**; 450 mg, 1.23 mmol). The title compound was obtained as a yellow solid (150 mg, 53%) after purification by column chromatography (hexane/ethyl acetate, 90:10). ^{1}H NMR ($CDCl_3$): δ = 8.66 (s, 1 H), 8.0 (s, 1 H), 7.89 (dd, 1 H), 7.73–7.78 (m, 3 H), 7.45 (s, 1 H),7.28–7.39 (m, 5 H), 2.06 (t, 8 H), 1.07 (m, 24 H), 0.8 (dt, 12 H), 0.64 (t, 8 H) ppm. ^{13}C NMR ($CDCl_3$): δ = 160.6, 152.6, 152.0, 151.4, 151.0, 145.0, 141.7, 141.2, 138.3, 135.6, 129.3, 127.4, 127.1, 125.9, 123.2, 121.5, 120.1, 119.7, 116.6, 102.2, 61.2, 55.4, 40.7, 31.9, 30.0, 24.1, 22.9, 15.6, 14.4 ppm. HRMS (+ve): *m*/*z* calcd. for $[C_{77}H_{100}N_2 + H]^+$ 1053.7886; found 1053.7882.

(N^2*E*,N^7*E*)-*N*^{2},*N*^{7}-Bis[(9,9-dihexyl-9*H*-fluoren-2-yl)methylene]-9*H*-fluorene-2,7-diamine (6): Obtained from 9,9-dihexyl-9*H*-fluorene-2-carboxaldehyde (**18**; 590 mg, 1.63 mmol) and 9*H*-fluorene-2,7-diamine (100 mg, 0.51 mmol). The title compound was obtained as a yellow solid (230 mg, 51%) after purification by column chromatography (hexane/ethyl acetate, 80:20). ^{1}H NMR ($CDCl_3$): δ = 8.66 (s, 1 H), 8.0 (s, 1 H), 7.9 (dd, 1 H), 7.78 (m, 3 H), 7.31–7.39 (m, 5 H), 4.10 (br. s, 2 H), 2.07 (t, 8 H), 1.06 (m, 24 H), 0.78 (dt, 12 H), 0.63 (t, 8 H) ppm. ^{13}C NMR ($CDCl_3$): δ = 160.4, 152.7, 151.5, 144.9, 144.0, 143.7, 141.8, 140.3, 136.4, 130.8, 129.3, 127.2, 126.9, 125.4, 123.0, 120.8, 120.6, 120.1, 118.1, 55.9, 55.8, 40.7, 37.3, 32.2, 29.6, 24.2, 22.9, 14.4 ppm. HRMS (+): *m*/*z* calcd. for $[C_{65}H_{76}N_2 + H]^+$ 885.6008; found 885.6004.

(*N*,*N*′*E*,*N*,*N*′*E*)-*N*,*N*′-[(9,9-Dihexyl-9*H*-fluorene-2,7-diyl)bis(methanylylidene)]bis(9,9-dihexyl-9*H*-fluoren-2-amine) (7): Obtained from 9,9-dihexyl-9*H*-fluoren-2-ylamine (**16**; 245 mg, 0.702 mmol) and 9,9-dihexyl-9*H*-fluorene-2,7-dicarbaldehyde (**20**; 98 mg, 0.219 mmol). The title compound was obtained as a yellow solid (130 mg, 89%) after purification by column chromatography (hexane/ethyl acetate, 70:30). ^{1}H NMR ($CDCl_3$): δ = 8.69 (s, 1 H), 8.05 (s, 1 H), 7.91 (dd, 2 H), 7.45 (dd, 2 H), 7.28–7.39 (m, 5 H), 2.06 (dt, 8 H), 1.10 (m, 24 H), 0.83 (dt, 12 H), 0.64 (br. s, 8 H) ppm. ^{13}C NMR ($CDCl_3$): δ = 160.3, 152.7, 152.5, 151.7, 151.2, 144.0, 141.2, 139.9, 136.4, 129.64, 127.2, 123.3, 123.2, 123.0, 121.0, 120.6, 119.9, 119.8, 116.5, 55.9, 55.6, 41.0, 40.8, 32.2, 32.0, 31.9, 30.4, 30.2, 29.7, 29.6, 24.2, 23.0, 14.5, 14.4 ppm. HRMS (+ve): *m*/*z* calcd. for $[C_{77}H_{100}N_2 + H]^+$ 1053.7886; found 1053.7884.

(N^2*E*,N^7*E*)-*N*^{2},*N*^{7}-Bis[(9*H*-fluoren-2-yl)methylene]-9,9-dihexyl-9*H*-fluorene-2,7-diamine (8): Obtained from 9,9-dihexyl-9*H*-fluoren-2-ylamine (**14**; 150 mg, 0.411 mmol) and 9*H*-fluorene-2-carbaldehyde (290 mg, 1.31 mmol). The title compound was obtained as an orange solid (110 mg, 37%) after purification by column chromatography (hexane/ethyl acetate, 80:20). ^{1}H NMR ($CDCl_3$): δ = 8.68 (s, 1 H), 8.23 (s, 1 H), 7.93 (dd, 3 H), 7.73 (s, 1 H), 7.61 (s, 1 H), 7.39 (dd, 2 H),7.28 (m, 2 H), 4.02 (br. s, 2 H), 2.04 (t, 2 H), 1.08 (m, 6 H), 0.8 (t, 3 H), 0.74 (t, 2 H) ppm. ^{13}C NMR ($CDCl_3$): δ = 160.4, 152.7, 151.5, 144.9, 144.0, 143.7, 141.8, 140.3, 136.4, 129.3, 127.2, 126.9, 125.4, 123.0, 120.9, 120.8, 120.6, 120.1, 118.1, 55.9, 55.8, 40.5, 37.4, 32.2, 30.2, 29.6, 24.2, 22.9, 14.4 ppm. HRMS (+ve): *m*/*z* calcd. for $[C_{53}H_{52}N_2 + H]^+$ 717.4130; found 717.4131.

(*E*)-*N*-[(9*H*-Fluoren-2-yl)methylene]-9*H*-fluoren-2-amine (9): To 9*H*-fluoren-2-ylamine (93.3 mg, 0.51 mmol) was added 9*H*-fluorene-2-carbaldehyde (100 mg, 0.51 mmol) in anhydrous ethanol, under N_2 and a catalytic amount of TFA. The solution was stirred at room temperature for 12 h until a yellow precipitate was formed. The mixture was filtered and the product was isolated as a yellow solid (183.7 mg, 100%). The product was insoluble in common deuterated solvents for NMR characterization and its subsequent characterization was not possible.

(*E*)-*N*-Benzylideneaniline (10): Obtained from benzaldehyde (50 mg, 0.471 mmol) and aniline (44 mg, 0.471). The title compound was obtained as an orange solid (30 mg, 35%) after purification by column chromatography (hexane/ethyl acetate, 70:30). ^{1}H NMR ($CDCl_3$): δ = 8.6 (s, 1 H), 7.98 (dd, 2 H), 7.53–7.55 (m, 3 H), 7.43 (dd, 2 H), 7.23–7.28 (s, 1 H) ppm. ^{13}C NMR ($CDCl_3$): δ = 160.6, 152.5, 152.2, 145.6, 137.0, 131.6, 129.6, 129.1, 129.0, 126.2, 121.2 ppm.

(*E*)-4-[(4-Cyanobenzylidene)amino]benzonitrile (11): Obtained from 4-formylbenzonitrile (100 mg, 0.72 mmol) and 4-aminobenzonitrile (90 mg, 0.72). The title compound was obtained as a white solid (158 mg, 95%) after purification by recrystallisation from ethanol. ^{1}H NMR ($CDCl_3$): δ = 8.77 (s, 1 H), 8.2 (d, 2 H), 7.97 (d, 2 H), 7.86 (d, 2 H), 7.46 (d, 2 H) ppm.

Supporting Information (see footnote on the first page of this article): Absorbance and fluorescence spectra, cyclic voltammograms, and ^{1}H and ^{13}C NMR spectra are provided.

Acknowledgments

The authors acknowledge financial support from the Natural Sciences and Engineering Research Council Canada for Discovery, Strategic Research, and Research Tools and Equipment. The Centre for Self-Assembled Chemical Structures and additional equipment funding from the Canada Foundation for Innovation are also acknowledged. W. G. S. also thanks the Alexander von Humboldt Foundation for funding that allowed the completion of this work.

[1] A. Bolduc, C. Mallet, W. G. Skene, *Sci. China Chem.* **2013**, *56*, 3–23.

[2] a) C. Wang, S. Shieh, E. LeGoff, M. G. Kanatzidis, *Macromolecules* **1996**, *29*, 3147–3156; b) C.-J. Yang, S. A. Jenekhe, *Chem. Mater.* **1991**, *3*, 878–887; c) J. E. G. Kuder, W. Harry, D. Wychick, *J. Org. Chem.* **1975**, *40*, 875–879; d) J. E. Kuder, H. W. Gibson, D. Wychick, *J. Org. Chem.* **1975**, *40*, 875–879.
[3] a) O. Thomas, O. Inganäs, M. R. Andersson, *Macromolecules* **1998**, *31*, 2676–2678; b) Z. Kucybala, I. Pyszka, B. Marciniak, G. L. Hug, J. Paczkowski, *J. Chem. Soc. Perkin Trans. 2* **1999**, 2147–2154; c) J. Skopalová, K. Lemr, M. Kotouèek, L. Èáp, P. Barták, *Fresenius J. Anal. Chem.* **2001**, *370*, 963–969.
[4] a) A. Iwan, M. Palewicz, A. Chuchmała, L. Gorecki, A. Sikora, B. Mazurek, G. Pasciak, *Synth. Met.* **2012**, *162*, 143–153; b) F.-C. Tsai, C.-C. Chang, C.-L. Liu, W.-C. Chen, S. A. Jenekhe, *Macromolecules* **2005**, *38*, 1958–1966; c) C.-L. Liu, W.-C. Chen, *Macromol. Chem. Phys.* **2005**, *206*, 2212–2222; d) A. a. Bolduc, S. p. Dufresne, W. G. Skene, *J. Mater. Chem.* **2012**, *22*, 5053–5064.
[5] a) H. T. Nicolai, A. Hof, P. W. M. Blom, *Adv. Funct. Mater.* **2012**, *22*, 2040–2047; b) M. C. Gather, A. Köhnen, K. Meerholz, *Adv. Mater.* **2011**, *23*, 233–248; c) M. Schäferling, *Angew. Chem.* **2012**, *124*, 3590; *Angew. Chem. Int. Ed.* **2012**, *51*, 3532–3554.
[6] a) A. N. Bourque, S. Dufresne, W. G. Skene, *J. Phys. Chem. C* **2009**, *113*, 19677–19685; b) S. Dufresne, S. A. P. Guarìn, A. Bolduc, A. N. Bourque, W. G. Skene, *Photochem. Photobiol. Sci.* **2009**, *8*, 796–804.
[7] a) P. Robert, A. Bolduc, W. G. Skene, *J. Phys. Chem. A* **2012**, *116*, 9305–9314; b) S. Dufresne, I. U. Roche, T. Skalski, W. G. Skene, *J. Phys. Chem. C* **2010**, *114*, 13106–13112; c) D. Tsang, M. Bourgeaux, W. G. Skene, *J. Photochem. Photobiol. A: Chem.* **2007**, *192*, 122–129.
[8] a) Y. Luo, M. Utecht, J. Dokić, S. Korchak, H.-M. Vieth, R. Haag, P. Saalfrank, *ChemPhysChem* **2011**, *12*, 2311–2321; b) J. Mielke, F. Leyssner, M. Koch, S. Meyer, Y. Luo, S. Selvanathan, R. Haag, P. Tegeder, L. Grill, *ACS Nano* **2011**, *5*, 2090–2097; c) T. W. Swaddle, H. Doine, S. D. Kinrade, A. Sera, T. Asano, T. Okada, *J. Am. Chem. Soc.* **1990**, *112*, 2378–2382; d) K. Maeda, K. A. Muszkat, S. Sharafi-Ozeri, *J. Chem. Soc. Perkin Trans. 2* **1980**, 1282–1287; e) J. W. Lewis, C. Sandorfy, *Can. J. Chem.* **1982**, *60*, 1720–1726; f) N. R. King, E. A. Whale, F. J. Davis, A. Gilbert, G. R. Mitchell, *J. Mater. Chem.* **1997**, *7*, 625–630.
[9] a) E. Fischer, Y. Frei, *J. Chem. Phys.* **1957**, *27*, 808–809; b) G. Wettermark, J. Weinstein, J. Sousa, L. Dogliotti, *J. Phys. Chem.* **1965**, *69*, 1584–1587.
[10] a) K. Li, B. Liu, *Polym. Chem.* **2010**, *1*, 252–259; b) G. Nie, H. Yang, J. Chen, Z. Bai, *Org. Electron.* **2012**, *13*, 2167–2176; c) A. Rostami, C. J. Wei, G. Guérin, M. S. Taylor, *Angew. Chem.* **2011**, *123*, 2107; *Angew. Chem. Int. Ed.* **2011**, *50*, 2059–2062; d) D. Thirion, M. Romain, J. Rault-Berthelot, C. Poriel, *J. Mater. Chem.* **2012**, *22*, 7149–7157; e) D. Thirion, J. l. Rault-Berthelot, L. Vignau, C. Poriel, *Org. Lett.* **2011**, *13*, 4418–4421; f) A. L. Fisher, K. E. Linton, K. T. Kamtekar, C. Pearson, M. R. Bryce, M. C. Petty, *Chem. Mater.* **2011**, *23*, 1640–1642; g) K. E. Linton, A. L. Fisher, C. Pearson, M. A. Fox, L.-O. Palsson, M. R. Bryce, M. C. Petty, *J. Mater. Chem.* **2012**, *22*, 11816–11825.
[11] a) N. Nijegorodov, V. Zvolinsky, P. V. C. Luhanga, *J. Photochem. Photobiol. A: Chem.* **2008**, *196*, 219–226; b) N. Nijegorodov, P. V. C. Luhanga, J. S. Nkoma, D. P. Winkoun, *Spectrochim. Acta Part A* **2006**, *64*, 1–5.
[12] a) Q. Zhao, S.-J. Liu, W. Huang, *Macromol. Chem. Phys.* **2009**, *210*, 1580–1590; b) F. Laquai, Y.-S. Park, J.-J. Kim, T. Basché, *Macromol. Rapid Commun.* **2009**, *30*, 1203–1231.
[13] S. Dufresne, W. G. Skene, *Acta Crystallogr., Sect. E* **2011**, *67*, o2302.
[14] U. Asawapirom, R. Güntner, M. Forster, T. Farrell, U. Scherf, *Synthesis* **2002**, 1136–1142.
[15] a) L. S. Rohwer, J. E. Martin, *J. Lumin.* **2005**, *115*, 77–90; b) A. G. Tweet, *Rev. Sci. Instrum.* **1963**, *34*, 1412–1417.
[16] a) C.-J. Yang, S. A. Jenekhe, *Macromolecules* **1995**, *28*, 1180–1196; b) C. L. Liu, W. C. Chen, *Macromol. Chem. Phys.* **2005**, *206*, 2212–2222.
[17] a) N. J. Turro, V. Ramamurthy, J. C. Scaiano, *Principles of Molecular Photochemistry: An Introduction*, University Science Books, Sausalito, **2009**; b) N. J. Turro, V. Ramamurthy, J. C. Scaiano, *Modern Molecular Photochemistry Of Organic Molecules*, University Science Books, **2010**.
[18] J. R. Lakowicz, *Principles of Fluorescence Spectroscopy*, 3rd ed., Springer, New York, **2006**.
[19] S. Barik, W. G. Skene, *Polym. Chem.* **2011**, *2*, 1091–1097.
[20] C. Mallet, M. Le Borgne, M. Starck, W. G. Skene, *Polym. Chem.* **2013**, *4*, 250–254.
[21] S. Barik, T. Bletzacker, W. G. Skene, *Macromolecules* **2012**, *45*, 1165–1173.
[22] H. Goerner, E. Fischer, *J. Photochem. Photobiol. A: Chem.* **1991**, *57*, 235–246.
[23] Y. Luo, S. Korchak, H.-M. Vieth, R. Haag, *ChemPhysChem* **2011**, *12*, 132–135.
[24] D. Gegiou, K. A. Muszkat, E. Fischer, *J. Am. Chem. Soc.* **1968**, *90*, 12–18.
[25] S. Dufresne, T. Skalski, W. G. Skene, *Can. J. Chem.* **2011**, *89*, 173–180.
[26] a) C. Wang, H. Dong, W. Hu, Y. Liu, D. Zhu, *Chem. Rev.* **2012**, *112*, 2208–2267; b) H. M. Koepp, H. Wendt, H. Stkehlow, *Z. Elektrochem.* **1960**, *64*, 483–491; c) J. Pommerehne, H. Vestweber, W. Guss, R. F. Mahrt, H. Bässler, M. Porsch, J. Daub, *Adv. Mater.* **1995**, *7*, 551–554.
[27] C. Chi, G. Wegner, *Macromol. Rapid Commun.* **2005**, *26*, 1532–1537.
[28] a) S. A. Pérez Guarìn, S. Dufresne, D. Tsang, A. Sylla, W. G. Skene, *J. Mater. Chem.* **2007**, *17*, 2801–2811; b) S. Barik, S. Friedland, W. G. Skene, *Can. J. Chem.* **2010**, *88*, 945–953.

Received: November 9, 2012
Published Online: March 15, 2013

